Liquefaction-Induced Underground Flow Failures in Gently-Inclined Fills Looser than Critical

Takaji Kokusho[1], Hazarika Hemanta[2], Tomohiro Ishizawa[3] and Shin-ichiro Ishibashi[4]

[1] Chuo University (Professor Emeritus), Tokyo, Japan
[2] Hemanta Hazarika, Kyushu University, Geo-disaster Prevention Engineering Research Laboratory, Fukuoka, Japan
[3] National Research Institute for Earth Science and Disaster Resilience, Tsukuba, Japan
[4] Nihon Chiken Company Ltd., Fukuoka, Japan

Abstract. In similar and unprecedented case histories during recent earthquakes in Hokkaido Japan, liquefied sand strangely flowed underground in gentle man-made fill slopes of a few percent gradient, leaving large surface depression behind. In both of them, a large amount of non-plastic fines was involved in loose fine fill sands. That particular sand with fines content $F_c \approx 35\%$ tested in undrained triaxial tests was found far more contractive with strain-softening and easier to flow than that of the same density deprived of fines. This strongly suggests that high fines content was the major cause of the strange flow failures because it destined the sand flowable on the contractive side of Steady State Line under sustained shear stress. Another series of cyclic simple shear tests on contractive sands with non-plastic fines under initial shear stress indicated that flow failure tends to occur in gentler slopes when the effective stress path comes across a yield line uniquely drawn from the origin on $\tau \sim \sigma_c'$ diagram irrespective of stress paths. Thus, a scenario to realize the unprecedented flow failures has been clarified based on the field observations and test results.

Keywords: Liquefaction, Flow, Gentle slope, Initial shear stress, Contractive, Nonplastic fines.

1 Introduction

Since 1964 when geotechnical engineers first recognized the significant effect of earthquake-induced liquefaction on infrastructures during the two earthquakes in Niigata and Alaska, typical failure modes familiar among engineers has been sand boils, soil settlement, lateral spreading, loss of bearing capacity and associated settlement and tilting of foundations relative to adjacent soils. Laboratory tests demonstrated that the failure occurs even in the dilative side of Steady State Line though flow type failure by sustained initial shear stress cannot occur there. The most of earthquake-induced liquefaction cases experienced since then seem to belong to this type.

However, unprecedented but similar failures occurred twice during recent earthquakes in Hokkaido, wherein liquefied sand strangely flowed underground in very

gentle man-made fill slopes of about 3% gradient, with no surface fissures and sand boils, leaving large ground depression behind with no surface disturbance.

Here, these two cases are first outlined to highlight their common features including geotechnical properties. Then, undrained triaxial test results on sand sampled from one of the sites are focused to discuss particularly on the role of non-plastic (NP) fines contained in the sand. Furthermore, the flow mechanism is discussed by revisiting torsional shear test results on similar fines-containing sand under initial shear stress again by focusing the role of NP fines in order to clarify the scenario how the unprecedented failures could occur under the given conditions.

2 Two Case Histories of Liquefaction Flow in Gentle Slopes

2.1 Sapporo Case

2018 Hokkaido Iburi-East earthquake (M=6.7) incurred unprecedented liquefaction damage in residential landfill in Satozuka, Kiyota-ward, Sapporo city about 50 km distant from the epicenter (Fig. 1 (a)). The horizontal peak ground acceleration (PGA) near the site was a little lower than 0.2 g with the predominant frequency 2.5~5 Hz and the duration of major motion around 20 seconds [1] (Fig. 1 (b)).

Considerable surface depression occurred locally in a residential landfill, the cross-sections of which are depicted in Fig. 1 (c). Former landscape of the site was undulated

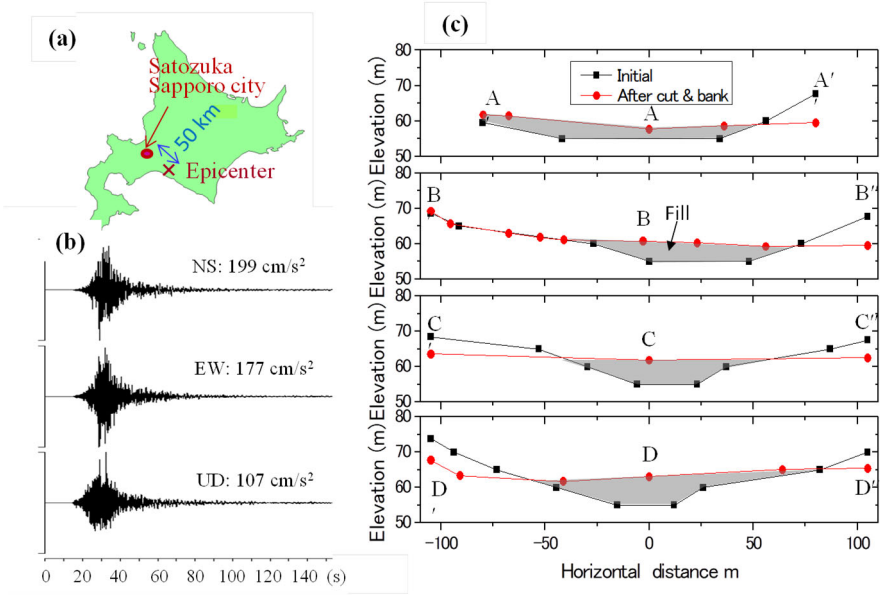

Fig. 1. 2018 Hokkaido Iburi-East earthquake and liquefied site Satozuka in Sapporo city (a), Acceleration records at K-NET Hiroshima 8 km from the site modified from NIED [1] (b), and Cross-section of Satozuka residential landfill (c).

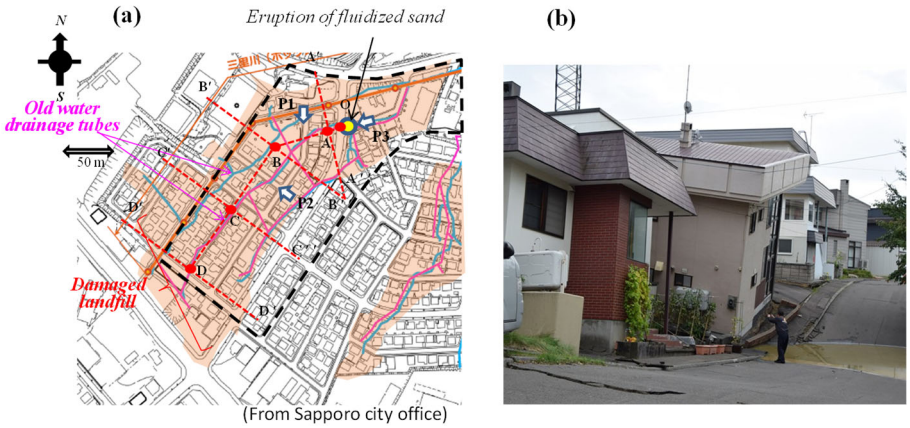

Fig. 2. Town map of damaged area with depression along OABCD (a), and Photograph of liquefaction-induced depression in residential land in Satozuka (b).

hills and lowlands of rice field in between. In early 1980s, the residential land development started by cutting hills (Pleistocene volcanic tuff) and filling lowlands in between with thickness 5~9 m. In post-earthquake soil investigations (Sapporo City Office 2018 [2]), surprisingly loose soil layers of SPT resistance $N \approx 1$ could be found not only at the depression but also far from it, probably because the landfill was of high fines content (F_c≈35%) and very poorly compacted originally.

Fig. 2 (a) shows the present map of damaged area including streets and houses, where the depression occurred about 3 m deep maximum, 20~30 m wide and 200 m long along Point O, A, B, C, D upslope in the shaded filled area. The original surface gradient along Line OD was 2.6% on average, downslope from D to O with the water level GL.-2 ~ -3 m. Huge volume of liquefied sand underneath the depression belt flowed underground laterally to Point O. In Fig. 2 (a), water drainage lines in old rice fields before landfilling are superposed which appear to be coincidental with the depression belt, leading to a suspicion that this might somehow help the depression occur.

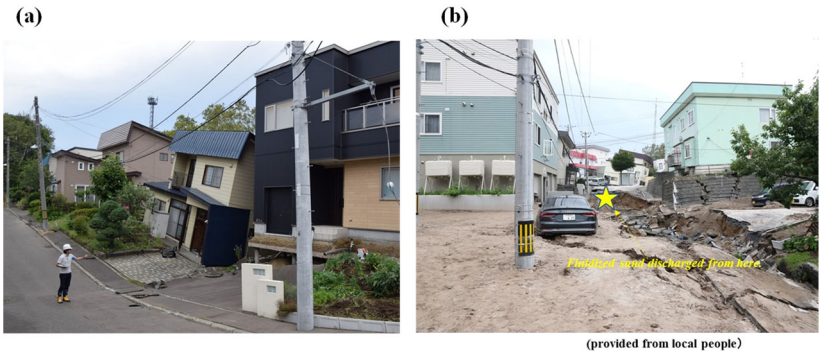

Fig. 3. (a) Large depression at P2 in Figure 2 (c), and (b) Sand ejection point where pavements were teared off violently and fluidized sand discharged and flowed downslope.

A number of independent houses along the ground depression belt were significantly influenced as photographed in Fig. 2 (b) and Fig.3 (a). Note that global building settlement occurred together with the depressed ground while no foundation settlement was observed relative to adjacent ground surface, quite different from normal liquefaction damage experienced so far. Neither fissures nor sand boils occurred in and around the depression. It was because liquefied sands were fluidized and flowed like a liquid exclusively underground all the way, and collectively ejected at a remote fill margin Point O in Fig.2 (a) into the air and went away as photographed in Fig. 3 (b).

2.2 Kitami Case

A similar liquefaction case had once occurred in Tanno-cho, Kitami city in Hokkaido, during the 2003 Tokachi-oki earthquake (M=8.0) as reported by Yamashita et al., (2005) [3] and Tsukamoto et al. (2009) [4], though it did not draw attention in general public because it was a rural farmland. The site was about 230 km away from the offshore hypocenter (Fig. 4 (a)), and the maximum acceleration nearby was only 0.055 g though the major motion lasted long about one minute (NIED 2018) (Fig. 4 (b)). Analogous to the Sapporo case, the farmland, artificially filled with loose volcanic sandy soil and gently inclined (about 3%), liquefied and left a great depression behind. However, the ground surface remained intact with no lateral displacement in furrows and no large fissures and sand boils in the subsided area (Fig. 4 (c)).

As shown in the air-photograph and plan view of Fig. 5 (a), (b), an area of 150 m long and 40~50 m wide subsided by 3.5 m maximum, and the downslope side was covered by sand ejecta containing NP fines (F_c=33%) spouted from four points and flowed downstream 1 km along a ditch. This again indicates considerable underground flowability of liquefied sand of maximum distance 150 m to the ejection points along an old shallow valley where the sand fill was 4~7 m thick and the water table 1~2 m deep. Unlike the Sapporo case, no drainage had been embedded in the downslope

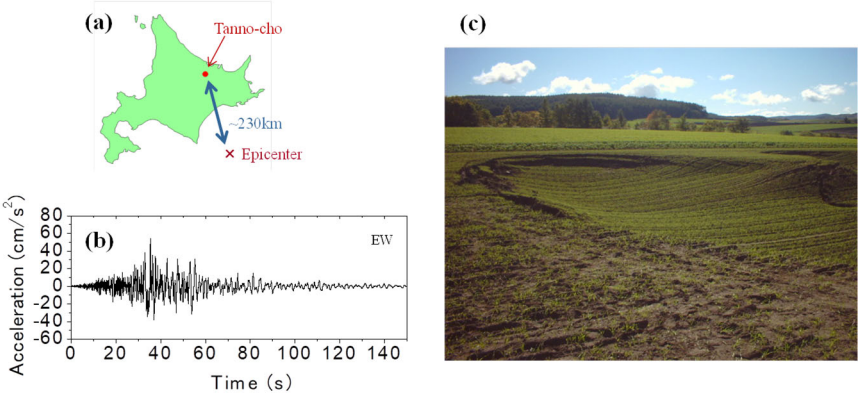

Fig. 4. Similar landfill failure in farmland in Kitami during 2003 Tokachi-oki earthquake: (a) Photo of ground depression, (b) Site and epicenter, and (c) Acceleration record K-NET Kitami (EW) 10 km from the site [1].

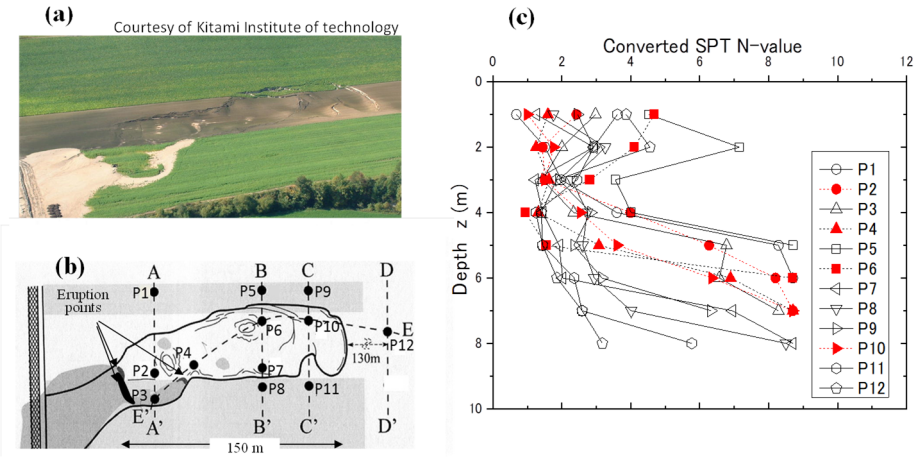

Fig. 5. Air-photograph (a) and Plan view with soil investigation points (Tsukamoto et al.2009 [4]) (b), and Penetration resistance versus depth (c) in landfill failure in Kitami.

direction (Yamashita 2019 [5]). Soil investigation after the earthquake using Swedish Weight Sounding (SWS) at many points in the figure indicated that SPT N-values converted from SWS was as loose as N=1 in the loosest portions both inside and outside of the depression area (Fig. 5 (c)).

2.3 Similarity of Two Cases

Fluidized sands at the above two cases sedimented in the downstream were sampled to investigate their physical properties. The grain-size curves of the two sands are illustrated in Fig. 6 (a), among which Samples **a, b, c** of the Sapporo sand show almost perfect coincidence; the average grain size was D_{50}=0.13 mm, uniformity coefficient C_u=25~35, fines content F_c≈35% and non-plastic (NP), despite that they were sampled at different sedimented area, indicating a good homogeneity of the liquefied sand.

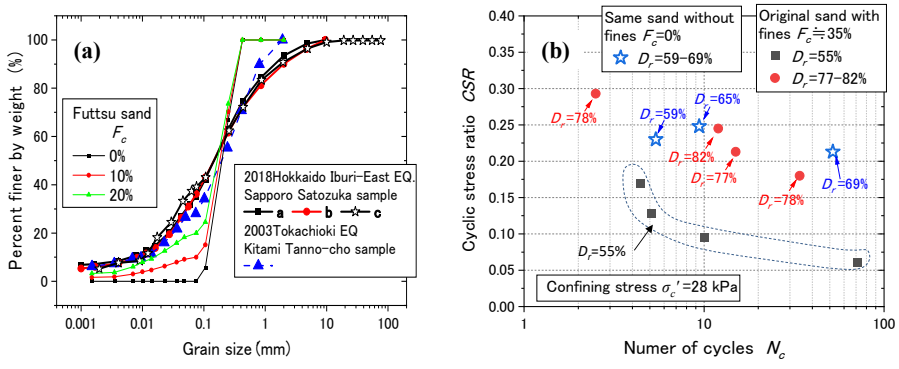

Fig. 6. Grain size curves of erupted sands in Sapporo and Kitami compared with Futtsu sand (a), and *CSR* versus N_c plots by undrained cyclic triaxial tests on Sapporo sand (b).

Furthermore, the Kitami sand was very similar in physical properties; D_{50}=0.2 mm, uniformity coefficient C_u=30, fines content F_c=33% and NP, all of that showed good similarity with the Sapporo sand, despite completely different locations. The specific soil particle densities were both extraordinarily low, ρ_s=2.26～2.28 t/m^3 in Sapporo and ρ_s=2.47 t/m^3 in Kitami, implying a mixture of large quantity of volcanic pumice (porous and easy to crush).

Thus, the two very analogous case histories of unprecedented liquefaction-induced underground flow failure obviously share common features; 1) Both occurred in gently inclined (≈3%) landfills of low density of N-value≈1 with shallow ground water, 2) Both accompanied neither ground surface fissures nor sand boils unlike normal liquefaction manifestations but considerable depressions of 3 m or deeper left behind liquefied sands traveling long distance downslope and spouting out collectively, and 3) the two sands share very similar physical properties among which NP fines contained more than F_c=30% seems to have had the remarkable effects on the flowability. Hence, the effect of NP fines is particularly focused as follows.

3 Undrained triaxial tests on Sapporo sand

In order to know the effect of NP fines on the soil behavior, undrained triaxial tests have been conducted on sampled Sapporo sand. Test specimens of 5 cm in diameter

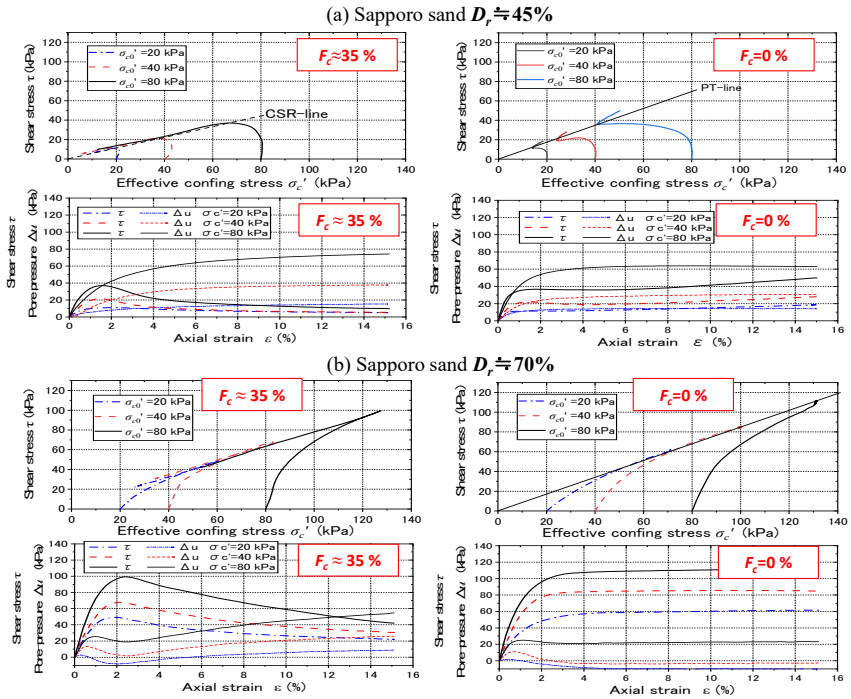

Fig. 7. Effective stress path (top) and stress versus strain curve (bottom) in undrained monotonic loading triaxial tests for sands of F_c≈35% and 0%: (a) D_r=45%, (b) D_r=70%.

and 10 cm in height were reconstituted by the moist-tamping method. Cyclic loading tests and monotonic loading tests were conducted to compare the results between the original sand and clean sand deprived of fines (smaller than 75 μm) from the original for relative densities $D_r \approx$ 50 to 80% after consolidation. The maximum and minimum void ratios to determine D_r were measured by the JGS standardized method (JGS) as e_{max}=2.231, e_{min}=1.268 and e_{max}=2.351, e_{min}=1.422, for the sands with and without fines, respectively.

Fig. 6 (b) depicts cyclic stress ratios (*CSR*) versus number of cycles for initial liquefaction (N_L) with solid dots obtained under effective confining stress of σ_c'=28kPa for the original Sapporo sand of relative densities D_r=55% and $D_r \approx$ 80% plotted with close symbols. CRR_{20} (*CSR* for N_L=20) seems to be low (less than 0.1 for D_r=55% and nearly 0.2 for $D_r \approx$ 80%) compared to normal sands of the same D_r-values. The open star symbols, the test results for the same sand of D_r=59~69% but deprived of all fines, obviously exhibit higher strength than the original sand of $D_r \approx$ 80%, indicating that the sand was more liquefiable because of the high content of NP fines.

Fig. 7 shows results of undrained monotonic loading triaxial tests in terms of effective stress paths ($\tau \sim \sigma_c'$) and stress/pore-pressure versus strain curves ($\tau \sim \varepsilon$ or $\Delta u \sim \varepsilon$) for the Sapporo sand of (a) D_r=45% and (b) 70%, respectively, in 3-stepwise initial effective confining stresses σ_c'=20, 40, 80 kPa. For (a) D_r=45%, the original sand ($F_c \approx$35%) on the left tends to be very contractive in the stress path undergoing monotonic decline of τ after taking peak values (when the stress paths cross a dashed CSR-line mentioned later) for all the σ_c'-values. Correspondingly, the stress -strain ($\tau \sim \varepsilon$) curves exhibit post-peak strain softening for higher σ_c' in particular.

In contrast, the same sand of D_r=45% of F_c=0% on the right behaves quite differently with a clear turning point (when the stress paths cross a solid PT line explained later) followed by strain-hardening, and no clear strain softening in the $\tau \sim \varepsilon$ curves is visible. For (b) D_r=70%, the stress paths initially behave dilatively with increasing τ to a peak and then take a sharp downturn in the original sand of $F_c \approx$35% on the left in all the confining stresses σ_c' presumably due to collapsibility of soils rich of pumice, and the $\sigma - \varepsilon$ curves have peaks followed by temporary decline. No such post-peak decline both in the stress paths and the $\tau \sim \varepsilon$ curves occur in the sand of F_c=0% on the right.

Thus, the inclusion of NP fines in the Sapporo sand considerably changes the undrained shear behavior from dilative to contractive for D_r=45% in particular. Such a remarkable change of dilatancy due to inclusion of fines may characterize not only the Sapporo sand but presumably the Kitami sand as well having great similarities in many respects.

As for in situ densities of the two sands, the relative density may roughly be estimated as $D_r \approx$ 20% from SPT $N \approx$1 for the ground depth of around 3 m (effective vertical overburden σ_v'=42 kPa) using the empirical formula; D_r=21{N/[(σ_v'/98) + 0.7]}$^{0.5}$) (Meyerhof, 1957 [6]). Though this formula was developed for clean sands without fines, the in situ D_r may well be assumed here to be lower than 45%, indicating that the sands were contractive enough in the light of the above test results.

4 Flow mechanism under initial shear by torsional tests

The effect of NP fines on the undrained cyclic loading failures under initial shear stress was previously discussed by Kokusho (2020) [7] based on a series of monotonic and cyclic torsional simple shear tests. The undrained tests were conducted on reconstituted Futtsu beach sand mixed with NP fines for isotropic effective confining stress of σ_c' =98 kPa. The grain size curve is compared with the case history sands in Fig. 6 (a), where it is similar to the present case history sands in mean grain size though more poorly-graded.

Effective stress paths ($\tau \sim \sigma_c'$) and stress~strain curves ($\tau \sim \gamma$) by undrained monotonic shearing are depicted in the top and bottom of Fig. 8 (a), respectively, for D_r=24~26%. The stress path for F_c=0% shows dilative response despite the very low density, wherein σ_c' and τ both increase after turning direction at a point PT corresponding to Phase Transformation (Ishihara et al., 1975 [8]). The associated $\tau \sim \gamma$ curve undergoes strain-hardening after yielding near the PT points. In contrast, the same sand with fines content F_c=10% and 20% exhibits contractive strain-softening behavior after taking peak stress shown with the arrows in the graph. For F_c=20% in particular, the stress path after taking the peak moves toward the origin of zero effective stress, while the $\tau \sim \gamma$ curve approaches to zero residual strength.

The response of the Futtsu sand by the torsional shear tests in Fig. 8 (a) may be compared to that of the Sapporo sand by the triaxial compression tests depicted in Fig. 7 despite the difference in test methods. The Sapporo sand of F_c=0% shows dilative response with no strain-softening behavior for both D_r≈70% and 45%, that is similar to the Futtsu sand of D_r=26%, F_c=0%. With fines content changing from F_c ≈0 to 35%,

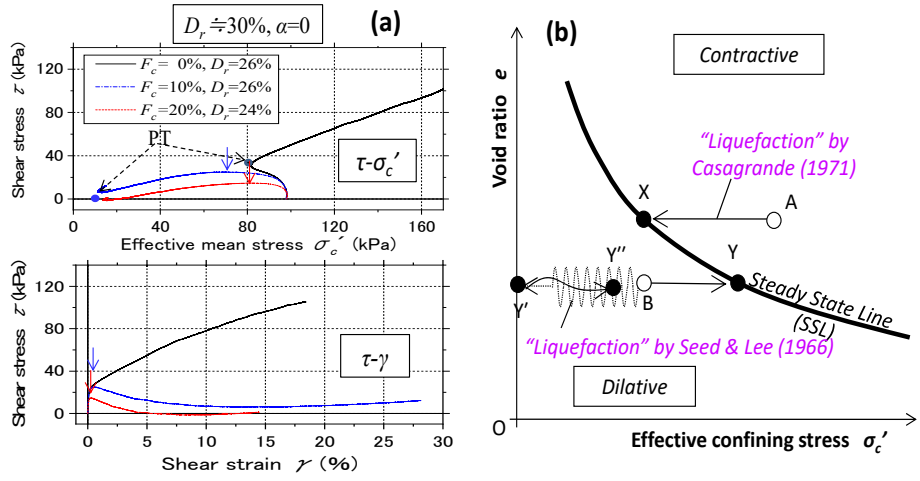

Fig. 8. Monotonic undrained torsional shear test results of varying F_c for D_r≈30%, σ_c' =98 kPa (a), and Conceptual chart of dilatancy characteristics on State Diagram with SSL and undrained loading path in contractive and dilative zones (b)

the Sapporo sand of D_r=45% becomes contractive with strain-softening, similar to the Futtsu sand of D_r≈30% with changing fines content from F_c=0% to 10% or 20%.

As a theoretical background of the above observations, a concept of State Diagram (Casagrande 1971 [9]) is shown in Fig. 8 (b) where the void ratio (e) versus effective confining stress (σ_c') plane is divided by Steady State Line (SSL) into contractive and dilative zones. A soil element on the contractive side of SSL if monotonically sheared in the undrained condition tends to be destabilized with decreasing σ_c' as Point **A** moves horizontally leftward to **X** on the SSL eventually. This corresponds seemingly to Sapporo sand of D_r=45%, F_c≈35% or Futtsu sand of D_r=24~26%, F_c=10, 20%. If the soil is sheared on the dilative side of SSL, the point **B** moves rightward with increasing σ_c' toward **Y** on SSL where no destabilization but strength increase occurs, corresponding to Sapporo and Futtsu sands of F_c=0% despite the almost the same D_r-values.

Obviously, this remarkable change of dilatancy is attributed to the change of F_c from around 35% (Sapporo sand) or 10~20% (Futtsu sand) to 0%. It was actually shown experimentally by Yang et al. (2006) [10], Papadopoulou and Tika (2008) [11], and Rahman and Baki (2011) [12] that SSL tends to move down-leftward with increasing F_c, changing the sand of the same density from dilative to contractive. Thus, it may well be inferred that the increase of NP fines changed the Sapporo sand from dilative to contractive in the same way as the Futtsu sand.

If sand is cyclically sheared, the point **B** even on the dilative side moves to the left due to negative dilatancy during cyclic loading unlike monotonic shearing, and reaches zero-effective stress at **Y′** as in Fig. 8 (b) under the zero-initial shear stress condition in level ground as Seed and Lee (1966) [13] first demonstrated in a cyclic triaxial liquefaction test. However, if sustained shear stress is working there, monotonic shearing starting from zero effective stress retranslates the point rightward to **Y″** reviving the

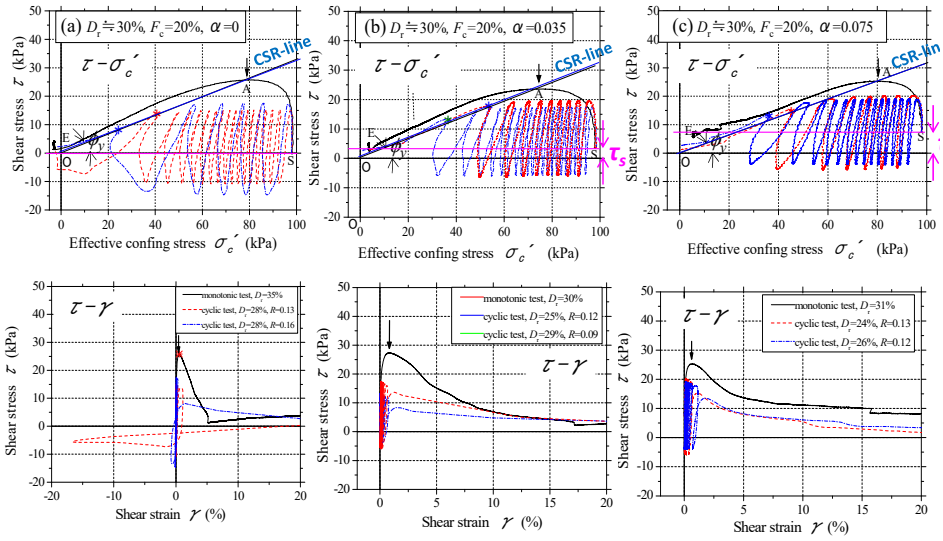

Fig. 9. Torsional shear test results of Futtsu sand in terms of τ~σ_c' (top) and τ~γ (bottom) for D_r≈30%, F_c=20% for 3 initial shear stress ratios: (a) α=0, (b) α=0.035, (c) α=0.075.

shear resistance. Thus, post-liquefaction flow-type failure by the initial shear stress is difficult to occur in the dilative zone.

In view of the above-mentioned case histories, it is interesting to clarify how the sands presumably on the contractive side of SSL can actually flow in undrained cyclic loading with cyclic stress amplitude (τ_d) under various initial shear stresses (τ_s). In Fig. 9 (a), (b), (c), the torsional shear test results with initial shear stress ratio $\alpha = \tau_s / \sigma_c'$ varying in three steps α=0, 0.035, 0.075, respectively, are addressed [7] in terms of $\tau \sim \sigma_c'$ (top) and the $\tau \sim \gamma$ (bottom) for $D_r \approx 30\%$, F_c=20%. The $\tau \sim \sigma_c'$ curves for the monotonic test (solid line) indicates the flow-type failure on the contractive side of SSL with decreasing σ_c' all the way from the start (S) to the end (E), where the shear stress τ takes peak at the point A marked with an arrow. The straight line OA drawn from the origin O with the angle ϕ_y represents the CSR-line defined by Vaid & Chern (1985) [14] as the line initiating shear stress decline. The associated $\tau \sim \gamma$ curves take clear stress peaks corresponding to the point A followed by strain-softening behavior leading to flow failure with monotonically declining shear strength to E.

In the cyclic loading tests with two different τ_d -values, the $\tau \sim \sigma_c'$ curves (dashed lines) in the top diagrams in Fig. 9 undergo gradual effective stress decrease (or pore-pressure buildup) to certain points marked with * where sudden strain-softening sets off leading to flow failure to the point E. In all the charts, the symbols * are positioned on or nearby the CSR-line AO defined by the corresponding monotonic tests. This indicates that the CSR-line represents a trigger of flow failure so that whenever the effective stress path comes across, flow failure starts irrespective of loading paths. In the bottom of Fig. 9, it is observed that corresponding strain exerted during cyclic loading is minor in magnitude, and the major strain is attributed to the flow failure by strain-softening. Also note that, except α=0 corresponding to non-flow cyclic failure in the absence of initial shear stress, the cases α=0.035 and 0.075 for very gentle slopes of gradient 3.5% or 7.5% belong to the stress reversal condition ($\tau_s < \tau_d$) wherein the pore pressure tends to build up faster than stress non-reversal condition ($\tau_d < \tau_s$).

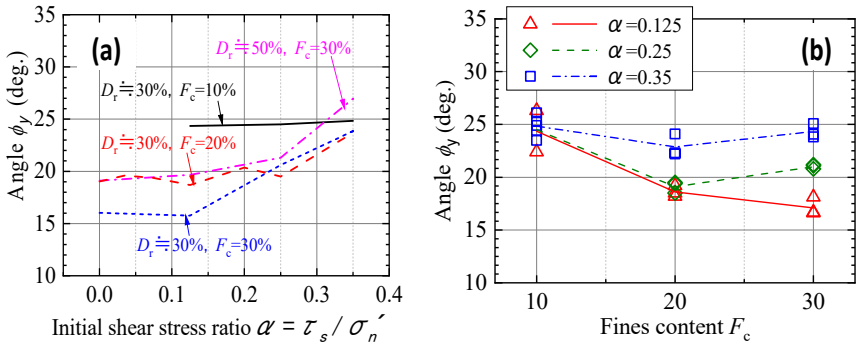

Fig.10. Angle of flow-triggering CSR-line : (a) plotted versus initial shear stress ratio α, and (b) plotted versus fines content F_c.

In the above discussion, the initiation of flow failure is obviously governed by the CSR-line with the angle ϕ_y with respect to the σ_c'-axis on the $\tau \sim \sigma_c'$ diagram. In Fig. 10 (a), the angle ϕ_y determined from a set of torsional shear tests on the Futtsu sand of D_r≈30%, 50% and F_c=10%, 20% and 30% are plotted versus the initial shear stress ratio α [7]. The ϕ_y -value tends to be essentially constant against α increasing from zero to a certain limit, thereafter followed individually by an ascending trend.

Fig. 10 (b) depicts the variations of ϕ_y against F_c for α=0.125, 0.25 and 0.35 for the same density D_r≈30%, wherein the averages of two to three ϕ_y -values for identical F_c-values are connected with straight lines. The ϕ_y -value tends to decrease remarkably with increasing F_c for smaller α in particular, while F_c makes little difference in ϕ_y for the high value of α=0.35. This indicates that flow-type failure tends to be triggered more easily with increasing F_c in gentler slopes (where the stress reversal is more likely to occur) than steeper slopes.

5 Possible Scenario of Underground Liquefaction Flow

The observations above on the flow failure mechanism of the Futtsu sand mixed with NP fines may well be applicable to in situ sands of Sapporo and Kitami considering the similarity of their physical properties. Thus, a possible scenario of the strange liquefaction-induced failures observed twice in recent decades may be described as follows.

1) In a gently inclined fill, very loose saturated sand containing large amount of NP fines and also crushable volcanic pumice on the contractive side of SSL was cyclically sheared during earthquakes.
2) When the stress path reached the CSR-line, the sand started strain-softening flow behavior under the influence of initial shear stress.
3) Due to unlimited flowability of highly contractive sand leading to ultra-low residual shear resistance, the sand mass started to flow underground due to slope gradient of 3% in downslope direction, and thereby induced suction in its upper boundary compressing the unsaturated non-liquefied surface layer by the atmospheric pressure.
4) Thus, neither ground fissures and sand boils nor relative settlement of building foundations into adjacent soils could occur in/around the depressions unlike normal liquefaction cases.
5) The liquefied sand mass could keep flowing underground, though with low speed because of small driving force in gentle slopes, and ejected downslope from weak points of the fills.
6) The above-mentioned suction seems to cancel pore-pressure buildup, recover effective stress, and thereby interrupt the sand to flow at least near the upper boundary of the liquefied sand. Nevertheless, the major portion of liquefied sand may have been able to flow, though more investigations are certainly needed to substantiate this mechanism more quantitatively.

6 Summary

Two case histories of strange liquefaction-induced flow failures during two recent earthquakes in Hokkaido, Japan are discussed. They are characterized as gently inclined (≈3%) landfills of low density with SPT N-value as low as unity in the extreme and shallow ground water. The failures accompanied neither ground fissures nor sand boiling but considerable depression belts of 3 m deep or more, as liquefied sand flowed underground in long distance and erupted downslope collectively. The two sands shared very similar physical properties; almost identical grain size curves, high contents of NP fines F_c>30%, and extraordinarily low soil particle density.

Undrained triaxial tests conducted on the sand sampled from the site (F_c>30%) indicated contractive behavior clearly different from that deprived of fines (F_c=0%). A series of torsional simple shear tests on similar sand demonstrated that flow failure sets off in contractive sand of high F_c when the effective stress path comes across the CSR-line starting from the origin with angle ϕ_y on the $\tau \sim \sigma_c'$ diagram uniquely determined for both monotonic and cyclic loading. The ϕ_y -value triggering the flow was found to decrease with increasing F_c particularly under small initial shear stress, indicating easier triggering of flow failure of high F_c-sands in gentle slopes in the stress-reversal condition.

Thus, a possible scenario of the two case histories has been constructed by focusing the significant role of NP fines in low density sands in triggering liquefaction-induced underground flow in gentle slopes leaving great depressions behind. In contrast to cyclic failures on the dilative side of SSL often observed so far, these case histories on the contractive side of SSL during earthquakes seem to have been scarce and worth documented and investigated more for mitigating similar future cases.

Acknowledgments

Ex-graduate students of Chuo University, Tokyo, Japan, Takuya Kusaka and Ryotaro Arai, who conducted a series of torsional shear tests and generated the valuable dataset incorporated in this paper are acknowledged for their great contribution. Ex-graduate students of Kyushu University Katsuya Ogo, who carried out the triaxial test of the Sapporo sand is also gratefully appreciated.

References

1. NIED: National Research Institute for Earth Science and Disaster Resilience, Tsukuba, Japan (2021).
2. Sapporo City Office: Publications for Forum to Residents on 2018 Earthquake Damage (2018).
3. Yamashita, S., Ito, Y., Hori T., Suzuki T, and Murata, Y.: Geotechnical properties of liquefied volcanic soil ground by 2003 Tokachi-Oki Earthquake, Published with Open Access under the Creative Commons BY-NC Licence by IOS Press (2005).

4. Tsukamoto, Y. Ishihara, K., Kokusho, T, Hara, T. and Tsutsumi, Y.: Fluidization and subsidence of gently sloped farming fields reclaimed with volcanic soils during 2003 Tokachi-oki earthquake in Japan, *Geotechnical Case History Volume*, Balkema, 109-118 (2009).
5. Yamashita, S: Personal communication (2019).
6. Meyerhof, G. G.: Discussion, Proc. 4th international Conference on SMFE, Vol.3, 110 (1957)
7. Kokusho, T.: Earthquake-induced flow liquefaction in fines-containing sands under initial shear stress by lab tests and its implication in case histories, *Soil Dynamics & Earthquake Engineering*, Elsevier, Vol. 130 (2020).
8. Ishihara, K., Tatsuoka, F. and Yasuda, S.: Undrained deformation and liquefaction of sand under cyclic stresses, *Soils and Foundations*, 15 (1), 29-44 (1975).
9. Casagrande, A.: On liquefaction phenomena, *Geotechnique*, London, England, XXI (3), 197-202 (1971).
10. Yang S., Lacasse S., and Sandven R.: Determination of the transitional fines content of mixtures of sand and non-plastic fines. GEOTECH. TEST. J., ASTM 29(2), 102-107 (2006).
11. Papadopoulou, A. and Tika, T.: The effect of fines on critical state and liquefaction resistance characteristics of non-plastic silty sands, *Soils & Foundations*, Japanese Geotechnical Society, 48, No.5, 713-725 (2008).
12. Rahman M.M., Lo, S.R., Baki, M.A.L.: Equivalent granular state parameters and undrained behavior of sand-fines mixtures. ACTA GEOTECHNICA, 6, 183194 (2011).
13. Seed H.B. and Lee, K.L.: Liquefaction of saturated sands during cyclic loading, *Journal of SMFD*, ASCE, 92 (6),105-134 (1966).
14. Vaid, Y. P. and Chern, J. C.: Cyclic and monotonic undrained response of saturated sands, Advances in the art of testing soils under cyclic conditions, *Proc.,* ASCE Convention, Detroit, Mich., 120-147 (1985).